Two-layer Bénard-Marangoni instability and the limit of transverse and longitudinal waves

A. Ye. Rednikov,[1,2] P. Colinet,[2] M. G. Velarde,[1] and J. C. Legros[2]
[1]*Instituto Pluridisciplinar, Universidad Complutense de Madrid, Paseo Juan XXIII, 1, Madrid 28040, Spain*
[2]*Université Libre de Bruxelles, MRC, Chimie-Physique EP, Code Postal 165, Avenue F.D. Roosevelt 50, Bruxelles 1050, Belgium*
(Received 27 December 1996; revised manuscript received 20 October 1997)

The oscillatory instability of a Bénard-Marangoni system composed of two liquid layers, of finite depth, separated by a deformable interface is considered. We show that in the limit of large Galileo and Marangoni numbers and small capillary number (boundary layer approximation), two modes of high-frequency interfacial excitation can be distinguished: transverse (capillary-gravity) waves and longitudinal waves.
[S1063-651X(98)02203-X]

PACS number(s): 47.20.Dr, 47.35.+i

I. INTRODUCTION

It is known that a temperature (concentration) gradient applied orthogonally to a horizontal liquid layer can induce instability of the motionless state, resulting in steady cellular convection (monotonic instability) or wave motion (oscillatory instability). Here we will restrict ourselves to the Marangoni mechanism of instability [1–3]. The role of the Marangoni (thermocapillary) effect in Bénard layers was theoretically established by Pearson [4]. For a layer with undeformable free surface and neglecting the properties of the overlying gas, he derived the condition for the onset of surface tension gradient-driven steady convection. As for oscillatory instability, it does not exist in Pearson's formulation, with an undeformable surface [5]. However, in multilayer systems overstability is possible even with undeformable interfaces [6–10]. Moreover, when the overlying fluid is a gas, overstability can also be obtained if a two-layer formulation is used, when the properties of the gas are taken into consideration [7,8]. On the other hand, in doubly diffusive systems, the oscillatory instability appears already in a one-layer formulation even with an undeformable surface [11–14]. However, if the interface deformability is taken into account, overstability becomes possible in Pearson's problem, as numerically shown by Takashima [15].

Physically, the undeformability of the free interface means that factors such as gravity and surface tension are strong enough to maintain the interface almost flat whatever flows and thermal inhomogeneities are induced. In terms of dimensionless parameters, this corresponds to a large enough Galileo number and a small enough capillary number. However, under the same conditions, large Galileo number and small capillary number, that bring about negligible surface deformation in Pearson's consideration, there exists a mode related to high-frequency surface oscillations that is analogous to capillary-gravity waves in the inviscid liquid layer [16]. In a viscous layer the Marangoni effect may be able to sustain these otherwise damped oscillations. Indeed, the results reported in the literature [17–21] and recent calculations [22] show that an oscillatory instability can be associated with this mode. Yet another type of high-frequency oscillatory mode of instability, a ''longitudinal'' mode, exists. This corresponds to oscillations mainly along the surface, in contrast to capillary-gravity waves (transverse mode) that correspond to essentially orthogonal oscillations of the deformable interface. The existence of longitudinal waves is intrinsically related to the Marangoni effect by the tangential balance of momentum. Just as the capillary-gravity wave keeps its identity (the oscillations are faster than their damping) only if the Galileo number is large enough and the capillary number is small enough, for the longitudinal wave we need the Marangoni number to be large enough (and have an appropriate sign). Here we will understand the longitudinal mode just in this (asymptotic) sense, although other interpretations also exist in the literature. Transverse and longitudinal waves at the interface separating two semi-infinitely deep liquid layers were also studied by Velarde and Chu [23–25].

The longitudinal waves were described by Lucassen-Reynders [26,27] when considering a free surface covered by surfactant. However, in their case the waves were strongly damped, as the relaxation time was of the order of the period of oscillations. When the longitudinal waves appear as a result of the temperature (concentration) gradient in the bulk, they are always only slightly damped, or even amplified. An important phenomenon here is the resonance between transverse and longitudinal waves when the mixing of modes occurs. This point has been studied by Earnshaw and collaborators [28,29].

In the present paper we consider the system of two finite-depth horizontal liquid layers separated by a deformable interface, assuming that the Galileo number is large, while the capillary number is small. We asymptotically study the high Marangoni number branches of the Bénard-Marangoni (thermocapillary) oscillatory instability, associated with transverse (capillary-gravity) and longitudinal waves. In Sec. II we formulate the linear stability problem in the boundary layer approximation. The (leading-order) dispersion relation is derived in Sec. III, providing the frequencies of transverse and longitudinal waves. Marginal stability conditions for both modes and the resonance between them are studied in Sec. IV. In Sec. V a detailed analysis of the resonance near the intersection of the marginal curves is carried out. Finally, we summarize our conclusions in Sec. VI.

II. FORMULATION OF THE LINEAR STABILITY PROBLEM

Consider a system of two liquid layers of finite depth and infinite horizontal extent, separated by a deformable inter-

face. The underlying layer (layer 1) rests on a flat rigid bottom. The overlying layer (layer 2) has lower density than the other to rule out Rayleigh-Taylor instability. The system is bounded above by a flat rigid top. The bottom and the top are maintained at different temperatures, inducing a linear temperature distribution inside the liquid layers. We look for linear oscillatory perturbations that can be sustained or amplified when the thermocapillary (Marangoni) effect is the only mechanism leading to instability.

Let us introduce dimensionless quantities using suitable scales, associated with the interface deformation (just like in the case of ideal, inviscid liquid), rather than scales related to thermal and viscous processes. Accordingly, we choose the following scales: h_1 for length, $(gh_1)^{1/2}$ for velocity, $(h_1/g)^{1/2}$ for time, $\rho_1 g h_1$ for pressure, and βh_1 for temperature, where h_1 is the depth of layer 1, g is the gravity acceleration, ρ_1 is the liquid density in layer 1, and β is the value of the imposed vertical temperature gradient there (we take $\beta>0$ if the heating is from above and $\beta<0$ otherwise). Correspondingly, the temperature gradient in layer 2 is $\kappa^{-1}\beta$, where κ is the ratio of thermal conductivities of the second and first liquids. Pressure and temperature refer to deviations of the corresponding quantities from their stationary distributions, linear with the vertical coordinate, in the motionless state.

In view of symmetry, we formulate our problem in two-dimensional geometry, with x and z being horizontal and vertical coordinates, respectively. The bottom of layer 1 is taken at $z=-1$, the top of layer 2 at $z=h$, and the interface is at $z=\eta(x,t)$. t denotes time and h is the ratio of the depths of the two layers. In the unperturbed state, the interface is at $z=0$.

Taking all these definitions and conventions into account, the linearized equations and boundary conditions (BC's) for the amplitudes of the normal modes $\exp(\lambda t+ikx)$ are

$$iku_j+w_{jz}=0, \tag{1}$$

$$\lambda u_j=-\delta_j^{(\rho)}ikp_j+\delta_j^{(\nu)}\left(\frac{\mathrm{Pr}}{G}\right)^{1/2}(u_{jzz}-k^2u_j), \tag{2}$$

$$\lambda w_j=-\delta_j^{(\rho)}p_{jz}+\delta_j^{(\nu)}\left(\frac{\mathrm{Pr}}{G}\right)^{1/2}(w_{jzz}-k^2w_j), \tag{3}$$

$$\lambda T_j+\delta_j^{(\kappa)}w_j=\frac{\delta_j^{(\chi)}}{(\mathrm{Pr}G)^{1/2}}(T_{jzz}-k^2T_j); \tag{4}$$

at $z=0$,

$$\lambda\eta=w_1=w_2, \tag{5}$$

$$u_1=u_2, \tag{6}$$

$$p_1-p_2=\eta\left(1-\rho+\frac{k^2}{B}\right)+2\left(\frac{\mathrm{Pr}}{G}\right)^{1/2}(w_{1z}-\rho\nu w_{2z}), \tag{7}$$

$$u_{1z}+ikw_1-\rho\nu(u_{2z}+ikw_2)+\frac{M}{(\mathrm{Pr}G)^{1/2}}ik(\eta+T_1)=0, \tag{8}$$

$$T_1+\eta=T_2+\kappa^{-1}\eta, \tag{9}$$

$$T_{1z}=\kappa T_{2z}; \tag{10}$$

at $z=-1$,

$$u_1=w_1=T_1=0; \tag{11}$$

and at $z=h$,

$$u_2=w_2=T_2=0, \tag{12}$$

with

$$G\equiv\frac{gh_1^3}{\nu_1\chi_1},\quad B\equiv\frac{\rho_1 gh_1^2}{\sigma},\quad M=-\frac{d\sigma}{dT}\frac{\beta h_1^2}{\rho_1\nu_1\chi_1},$$

$$h\equiv\frac{h_2}{h_1},\quad \mathrm{Pr}\equiv\frac{\nu_1}{\chi_1},\quad \rho\equiv\frac{\rho_2}{\rho_1},\quad \nu\equiv\frac{\nu_2}{\nu_1},\quad \chi\equiv\frac{\chi_2}{\chi_1},$$

$$\kappa\equiv\frac{\kappa_2}{\kappa_1},$$

$$\delta_j^{(\rho)}=\begin{cases}1 & \text{for } j=1\\ \rho^{-1} & \text{for } j=2,\end{cases}\qquad \delta_j^{(\nu)}\equiv\begin{cases}1 & \text{for } j=1\\ \nu & \text{for } j=2,\end{cases}$$

$$\delta_j^{(\chi)}\equiv\begin{cases}1 & \text{for } j=1\\ \chi & \text{for } j=2,\end{cases}\qquad \delta_j^{(\kappa)}\equiv\begin{cases}1 & \text{for } j=1\\ \kappa^{-1} & \text{for } j=2.\end{cases}$$

The subscripts $j=1,2$ refer to the quantities in layers 1 and 2, respectively. We also denote by η, u_j, w_j, p_j, T_j $(j=1,2)$ the (amplitudes of) interface deformation and horizontal and vertical components of the velocity field, pressure, and temperature, respectively. The subscript z refers to the corresponding derivative. $h_j, \rho_j, \nu_j, \chi_j, \kappa_j$ $(j=1,2)$ are the depths of the layers, densities, kinematic viscosities, thermal diffusivities, and conductivities, respectively. Symbols without subscripts refer to the ratios of the corresponding properties, always taken of layer 2 to that of layer 1, as defined above. σ is the interfacial tension. The Prandtl number Pr, Galileo number G, *static* Bond number B, and Marangoni number M have been defined using the properties of layer 1. The coefficients δ have been introduced to condense notation.

Equation (1) is the continuity equation. Equations (2) and (3) are the horizontal and vertical components of the linearized Navier-Stokes equation, while Eq. (4) is the heat equation. BCs (5) and (6) are the kinematic and no-slip conditions at the interface, respectively. BCs (7) and (8) account for the normal and tangential stress balances. The continuity of temperature and heat flux across the interface is expressed in BCs (9) and (10).

The problem (1)–(12) is solved asymptotically assuming that Pr, B, all material ratios, and the parameter $1-\rho>0$ are of order unity, while Galileo and Marangoni numbers are large. Thus the capillary number B/G is small. As we will find later on, the most general asymptotics corresponds to the Marangoni and Galileo numbers being of the same order of magnitude. This justifies our neglect of buoyancy. Indeed, the density variations due to thermal expansion of liquid are usually much smaller than the density (i.e., $\alpha\beta h_1\ll 1$, where α is the thermal expansion coefficient), hence the Rayleigh

number $R \equiv \alpha\beta h_1 G \ll G \sim M$. Thus this effect proves to be a negligible correction in all cases we deal with in the present paper.

The fact that G is considered large has consequences on the expected structure of the solution of the problem (1)–(12). Indeed, in the main bulk the dissipative effects are negligibly small and the flow can be considered irrotational. Vorticity appears only in the boundary layers at the rigid bottom or top, where the no-slip condition must be satisfied, and at the free interface, where the tangential (Marangoni) stresses are present. As Pr is of order unity, as well as the property ratios, the thermal boundary layers coincide with the viscous ones. The boundary layers are in general characterized by a sharp (as compared to the main bulk) change of the functions u, w, p, and T with the vertical coordinate, z. Using Eqs. (2)–(4), we find that the thickness of the boundary layers is of order $G^{-1/4}$. Accordingly, we introduce the smallness parameter

$$\epsilon \equiv \left(\frac{\mathrm{Pr}}{G}\right)^{1/4} \ll 1 \tag{13}$$

and the variables

$$\overline{z} = \frac{z}{\epsilon}$$

in the interface boundary layer,

$$\widetilde{z}_1 = \frac{z+1}{\epsilon}$$

in the bottom boundary layer, and

$$\widetilde{z}_2 = \frac{h-z}{\epsilon}$$

in the top boundary layer.

We look for the solution separately in each one of these regions and subsequently match them. This approach (the method of matched asymptotic expansions) is standard practice in problems where the smallness parameter affects the highest-order derivative [30].

Rewriting the problem (1)–(12) for each one of the three regions, we get ($j=1,2$) the following. (a) In the main bulk,

$$iku_j + w_{jz} = 0, \tag{14}$$

$$\lambda u_j = -\delta_j^{(\rho)} ikp_j + \epsilon^2 \delta_j^{(\nu)} (u_{jzz} - k^2 u_j), \tag{15}$$

$$\lambda w_j = -\delta_j^{(\rho)} p_{jz} + \epsilon^2 \delta_j^{(\nu)} (w_{jzz} - k^2 w_j), \tag{16}$$

$$\lambda T_j + \delta_j^{(\kappa)} w_j = \epsilon^2 \frac{\delta_j^{(\chi)}}{\mathrm{Pr}} (T_{jzz} - k^2 T_j). \tag{17}$$

(b) In the bottom and top boundary layers,

$$\epsilon iku_j + (-1)^{j+1} w_{j\widetilde{z}_j} = 0, \tag{18}$$

$$\lambda u_j = -\delta_j^{(\rho)} ikp_j + \delta_j^{(\nu)} u_{j\widetilde{z}_j\widetilde{z}_j} - \epsilon^2 \delta_j^{(\nu)} k^2 u_j, \tag{19}$$

$$\epsilon\lambda w_j = -(-1)^{j+1} \delta_j^{(\rho)} p_{j\widetilde{z}_j} + \epsilon \delta_j^{(\nu)} w_{j\widetilde{z}_j\widetilde{z}_j} - \epsilon^3 \delta_j^{(\nu)} k^2 w_j, \tag{20}$$

$$\lambda T_j + \delta_j^{(\kappa)} w_j = \frac{\delta_j^{(\chi)}}{\mathrm{Pr}} T_{j\widetilde{z}_j\widetilde{z}_j} - \epsilon^2 \frac{\delta_j^{(\chi)}}{\mathrm{Pr}} k^2 T_j. \tag{21}$$

At $\widetilde{z}_j = 0$,

$$u_j = w_j = T_j = 0. \tag{22}$$

(c) In the interface boundary layer,

$$\epsilon iku_j + w_{j\overline{z}} = 0, \tag{23}$$

$$\lambda u_j = -\delta_j^{(\rho)} ikp_j + \delta_j^{(\nu)} u_{j\overline{z}\,\overline{z}} - \epsilon^2 \delta_j^{(\nu)} k^2 u_j, \tag{24}$$

$$\epsilon\lambda w_j = -\delta_j^{(\rho)} p_{j\overline{z}} + \epsilon \delta_j^{(\nu)} w_{j\overline{z}\,\overline{z}} - \epsilon^3 \delta_j^{(\nu)} k^2 w_j, \tag{25}$$

$$\lambda T_j + \delta_j^{(\kappa)} w_j = \frac{\delta_j^{(\chi)}}{\mathrm{Pr}} T_{j\overline{z}\,\overline{z}} - \epsilon^2 \frac{\delta_j^{(\chi)}}{\mathrm{Pr}} k^2 T_j. \tag{26}$$

At $\overline{z} = 0$,

$$\lambda \eta = w_1 = w_2, \tag{27}$$

$$u_1 = u_2, \tag{28}$$

$$p_1 - p_2 = \eta\left(1 - \rho + \frac{k^2}{B}\right) + 2\epsilon w_{1\overline{z}} - 2\epsilon\rho\nu w_{2\overline{z}}, \tag{29}$$

$$u_{1\overline{z}} + \epsilon ikw_1 - \rho\nu(u_{2\overline{z}} + \epsilon ikw_2) + \frac{M\epsilon^3}{\mathrm{Pr}} ik(\eta + T_1) = 0, \tag{30}$$

$$T_1 + \eta = T_2 + \kappa^{-1}\eta, \tag{31}$$

$$T_{1\overline{z}} = \kappa T_{2\overline{z}}. \tag{32}$$

To solve the problem (14)–(32), all components of the function $f_j = (u_j, w_j, p_j, T_j)$ are expanded in power series of ϵ:

$$f_j(z) = f_{j0} + \epsilon f_{j1} + \epsilon^2 f_{j2} + \cdots \tag{33}$$

in the main bulk,

$$f_j(\overline{z}) = \overline{f_{j0}} + \epsilon\overline{f_{j1}} + \epsilon^2\overline{f_{j2}} + \cdots \tag{34}$$

in the interface boundary layer, and

$$f_j(\widetilde{z}_j) = \widetilde{f}_{j0} + \epsilon\widetilde{f}_{j1} + \epsilon^2\widetilde{f}_{j2} + \cdots \tag{35}$$

in the bottom and top boundary layers. The only exception is the function u_j in the interface boundary layer, which is sought in the form

$$u_j = \epsilon^{-1}\overline{u_{j(-1)}} + \overline{u_{j0}} + \epsilon\overline{u_{1j}} + \epsilon^2\overline{u_{j2}} + \cdots, \tag{36}$$

i.e., starting with the term of order ϵ^{-1}. The reason for this choice will be provided later on.

In principle, the parameters η and λ must be also represented in the form of expansions with ϵ, e.g.,

$$\lambda=\lambda_0+\epsilon\lambda_1+\cdots . \tag{37}$$

However, as they are simply constants (rather than functions of z), we may regard them at each step as containing the sufficient number of approximations. As for λ, the representation (37) will be used only in the final results, to avoid cumbersome intermediate calculations.

After substituting Eqs. (33)–(36) into Eqs. (14)–(32) we get a hierarchy of linear problems corresponding to ϵ^n ($n=-1,0,1,...$). At each step a solvability condition must be satisfied, hence providing a linear dispersion relation. Note that if η and λ were also expanded with ϵ, there would be a hierarchy of dispersion relations corresponding to each approximation in ϵ. As they are not expanded here, there will instead be a single dispersion relation, but containing terms of different orders in ϵ.

III. TRANSVERSE AND LONGITUDINAL WAVES

A. Zeroth-order approximation to the dispersion relation

In the main bulk, using Eqs. (14)–(16), we get

$$p_{10}=c_1\exp(kz)+c_2\exp(-kz), \tag{38}$$

$$u_{10}=-\frac{ik}{\lambda}[c_1\exp(kz)+c_2\exp(-kz)], \tag{39}$$

$$w_{10}=-\frac{k}{\lambda}[c_1\exp(kz)-c_2\exp(-kz)], \tag{40}$$

$$p_{20}=c_3\exp(kz)+c_4\exp(-kz), \tag{41}$$

$$u_{20}=-\frac{ik}{\rho\lambda}[c_3\exp(kz)+c_4\exp(-kz)], \tag{42}$$

$$w_{20}=-\frac{k}{\rho\lambda}[c_3\exp(kz)-c_4\exp(-kz)], \tag{43}$$

where $c_1,\ldots,c_4$ are constants of integration, yet to be determined. In the bottom and top boundary layers, Eq. (18) yields that $\tilde{w}_{j0}$ ($j=1,2$) are constants. Then, according to BC (22), $\tilde{w}_{10}=\tilde{w}_{20}=0$. The matching conditions between $\tilde{w}_{j0}$ and w_{j0} yield

$$c_1\exp(-k)=c_2\exp(k), \tag{44}$$

$$c_3\exp(kh)=c_4\exp(-kh). \tag{45}$$

In the interface boundary layer, using Eq. (25), we get that $\overline{p_{j0}}$ ($j=1,2$) are constants. Then using BC (29) and the conditions of matching between p_{j0} and $\overline{p_{j0}}$ we obtain

$$c_1+c_2-c_3-c_4=\eta\left(1-\rho+\frac{k^2}{B}\right). \tag{46}$$

Also in the interface boundary layer, Eq. (24) yields

$$\overline{u_{1(-1)}}=c_5\exp(\sqrt{\lambda}\overline{z}), \tag{47}$$

$$\overline{u_{2(-1)}}=c_6\exp(-\sqrt{\lambda}\nu^{-1/2}\overline{z}), \tag{48}$$

where c_5 and c_6 are constants and $\sqrt{\lambda}$ is taken with a positive real part. Using BC (28) we obtain

$$c_5=c_6. \tag{49}$$

Then using Eq. (23) and BC (27) we get

$$\overline{w_{10}}=\frac{ikc_5}{\sqrt{\lambda}}[1-\exp(\sqrt{\lambda}\overline{z})]+\lambda\eta, \tag{50}$$

$$\overline{w_{20}}=\frac{ikc_6}{\sqrt{\lambda}}\nu^{1/2}[\exp(-\sqrt{\lambda}\nu^{-1/2}\overline{z})-1]+\lambda\eta. \tag{51}$$

Now we use the matching conditions between w_{j0} and $\overline{w_{j0}}$ that gives

$$\frac{k}{\lambda}(c_2-c_1)-\frac{ik}{\sqrt{\lambda}}c_5=\lambda\eta, \tag{52}$$

$$\frac{k}{\rho\lambda}(c_4-c_3)+\frac{ik}{\sqrt{\lambda}}\nu^{1/2}c_6=\lambda\eta. \tag{53}$$

It appears clear why the expansion (36) for the horizontal velocity in the interface boundary layer needs to start with the term of order ϵ^{-1}. Otherwise we would get that $\overline{w_{j0}}$ ($j=1,2$) are just constants in the interface boundary layer [in view of Eq. (23)]; hence other possible solutions would be lost [such as Eq. (63), see below]. Note that owing to the no-slip boundary condition in the bottom and top boundary layers the expansion for the horizontal velocity must start with the same order as the expansion in the main bulk. Eliminating the coefficients $c_1,\ldots,c_5$ in the system of equations (44)–(46), (49), (52), and (53), we get

$$\begin{aligned}&-ik\sqrt{\lambda}[\rho\nu^{1/2}\coth(kh)-\coth(k)]c_6\\&\quad+[\rho\coth(kh)+\coth(k)](\lambda^2+\omega_0^2)\eta\\&\quad=0,\end{aligned} \tag{54}$$

with

$$\omega_0^2\equiv k\frac{1-\rho+k^2/B}{\rho\coth(kh)+\coth(k)}. \tag{55}$$

Let us now proceed to the temperature field. The solution in the interface boundary layer can be obtained in a closed form without referring to the main bulk and wall boundary layer solutions. Thus, provided the temperature gradient in the unperturbed state remains unchanged, the boundary layer approximation results do not depend on the particular form of the temperature boundary condition at the rigid bottom and top.

According to Eq. (26), taking Eqs. (50) and (51) into account, the zeroth-order solution approximation in the interface boundary layer is

$$\begin{aligned}\overline{T_{10}}=&-\eta-\frac{ikc_5}{\lambda\sqrt{\lambda}}-\frac{ikc_5}{\lambda\sqrt{\lambda}}\frac{\mathrm{Pr}}{1-\mathrm{Pr}}\exp(\sqrt{\lambda}\overline{z})\\&+c_7\exp(\sqrt{\lambda}\,\mathrm{Pr}^{1/2}\overline{z}),\end{aligned} \tag{56}$$

$$\overline{T_{20}} = -\kappa^{-1}\eta + \frac{ikc_6}{\lambda\sqrt{\lambda}}\,\nu^{1/2}\kappa^{-1} + \frac{ikc_6}{\lambda\sqrt{\lambda}}\,\nu^{1/2}\kappa^{-1}\,\frac{\mathrm{Pr}}{\chi\nu^{-1}-\mathrm{Pr}}\exp(-\sqrt{\lambda}\,\nu^{-1/2}\overline{z}) + c_8\exp(-\sqrt{\lambda}\,\mathrm{Pr}^{1/2}\chi^{-1/2}\overline{z}). \tag{57}$$

The coefficients c_7 and c_8 are found using BC (31) and (32). Then we use the last BC (30), which in the leading-order approximation considered here becomes

$$u_{1(-1)\overline{z}} - \rho\nu u_{2(-1)\overline{z}} + mik(\eta + T_{10}) = 0, \tag{58}$$

where, for convenience, a *modified* Marangoni number

$$m \equiv \frac{M\epsilon^4}{\mathrm{Pr}} \tag{59}$$

has been introduced. This quantity m is the inverse of the *dynamic* Bond number. Substituting Eqs. (47), (48), and (56) into Eq. (58), we obtain

$$(1+\rho\nu^{1/2})c_6 + \frac{mk^2}{\lambda^2}\,\frac{\chi^{1/2}\nu^{-1/2}-1}{(1+\kappa\chi^{-1/2})(1+\mathrm{Pr}^{1/2})(\chi^{1/2}\nu^{-1/2}+\mathrm{Pr}^{1/2})}\,c_6 = 0. \tag{60}$$

The constant c_6 is retained here, on the one hand, for its use in the solvability condition in the following subsection [in particular, Eq. (60) can be satisfied by $c_6=0$] and, on the other hand, to help the reconstitution with the corresponding first-order equation in Sec. IV.

B. Analysis and discussion of mode frequencies

The solvability condition demands the existence of a nontrivial solution for the coefficients c_6 and η of the system (54) and (60). It yields a vanishing determinant, i.e.,

$$(\lambda^2+\omega_0^2)\left(1+\frac{mk^2}{\lambda^2}\times\frac{\chi^{1/2}\nu^{-1/2}-1}{(1+\rho\nu^{1/2})(1+\kappa\chi^{-1/2})(1+\mathrm{Pr}^{1/2})(\chi^{1/2}\nu^{-1/2}+\mathrm{Pr}^{1/2})}\right) = 0. \tag{61}$$

Eq. (61) possesses two solutions:

$$\lambda^2 = -\omega_0^2 \tag{62}$$

and

$$\lambda^2 = -\frac{mk^2(\chi^{1/2}\nu^{-1/2}-1)}{(1+\rho\nu^{1/2})(1+\kappa\chi^{-1/2})(1+\mathrm{Pr}^{1/2})(\chi^{1/2}\nu^{-1/2}+\mathrm{Pr}^{1/2})}. \tag{63}$$

Thus we find that two different modes exist. The first one (62) is just the mode that appears in ideal, inviscid, liquid layers and accounts for capillary-gravity waves [16]. The second one (63) is due to the Marangoni effect and has no analog in the case of an inviscid liquid. Unlike the first mode, the second mode is not always oscillatory. Indeed, it is oscillatory only if the right-hand side of Eq. (63) is negative, i.e., if $m(1-\chi^{1/2}\nu^{-1/2})<0$. For liquids with normal interfacial tension dependence on temperature, i.e., whose value decreases with the increase of temperature, the second mode is oscillatory when $\chi<\nu$ and the heating is from above or when $\chi>\nu$ and the heating is from below.

The first mode is a transverse interfacial vibration since capillary-gravity waves are intrinsically related to interface deformations. The second mode corresponds to oscillations along the surface due to the Marangoni effect, hence the coinage ''longitudinal'' wave [26]. Returning to dimensional variables, expression (63) does not contain quantities related to surface deformation (g and σ). It does not contain the layer depths either. Thus the result (63) does not depend on whether the surface is deformable ($M\sim G$) or not ($M \ll G$). The only condition of its validity is $M\gg 1$; hence the time scale associated with longitudinal oscillations

$$\frac{\rho_1 h_1^2}{-d\sigma/dT\beta}$$

is shorter than the viscous and thermal time scales. (Note that in the estimations such as $M\gg 1$ we tacitly mean the absolute value of M.)

The most general case for $M\gg 1$, $G\gg 1$ is the case $M\sim G$ ($m\sim 1$), when the frequencies of both modes are about the same. It is worth noting that, although a nonvanishing interface deformation accompanies the second mode at $M\sim G$, it still clearly manifests its longitudinal character. Indeed, for the second mode there exists a strong horizontal component of the velocity field in the interface boundary layer that is $1/\epsilon$ times stronger than its corresponding value in the main bulk. For the first mode, in view of Eqs. (49), (54), and (62), the constants c_5 and c_6 are equal to zero; hence the velocity field is everywhere of the same order. The fact that the leading-order result (63) does not depend on layer depths, as already mentioned in the preceding paragraph, is just a consequence of the predominance of the longitudinal motion near the interface.

There exists a combination of the parameters such that the frequencies defined by Eqs. (62) and (63) become equal to each other. This corresponds to the resonance of the modes. It occurs for the following value of the *modified* Marangoni number:

$$m_{\mathrm{res}} = \frac{(1+\rho\nu^{1/2})(1+\kappa\chi^{-1/2})(1+\mathrm{Pr}^{1/2})(\chi^{1/2}\nu^{-1/2}+\mathrm{Pr}^{1/2})}{\chi^{1/2}\nu^{-1/2}-1}\,\frac{\omega_0^2}{k^2}. \tag{64}$$

As one can see from Eqs. (62) and (63), the eigenvalues for both modes tend to zero as k approaches zero. Thus the boundary layer approximation is not valid if k is too small or the waves are too long. Indeed, due to the lowering in oscillation frequency in the long-wave region, their characteristic time scale is no longer shorter than the viscous and thermal time scales. Let us estimate the value of k for which the boundary layer approach breaks down. In accordance with

the boundary layer exponents of, e.g., Eqs. (47) and (48), the condition is $\sqrt{\lambda}\sim\epsilon$. Taking Eqs. (62) and (63) into account, we get $k\sim\epsilon^2$, or recalling Eq. (13), $k\sim G^{-1/2}$ (for the second mode it should be $k\sim M^{-1/2}$ if we do not assume $m\sim 1$). Thus we have to demand that $k\gg G^{-1/2}$. On the other hand, there is also a limitation from above, i.e., from the side of large k or short waves. This limitation is related to the fact that in the short-wave region the penetration k^{-1} of the potential part of the flow inside the layer decreases faster at $k\to\infty$ than that of the rotational part $\epsilon/\sqrt{\lambda}$. The boundary layer approximation is valid only if the former is much larger than the latter. For the capillary-gravity mode, this yields the condition $k\ll\epsilon^{-4}$ or $k\ll G$ (if $B\sim 1$). We can also make the corresponding estimate for the longitudinal mode. Note that with the increase of G and M, the domain of validity grows both towards the long-wave region and towards the short-wave region.

The zeroth-order solution has provided the frequencies of transverse and longitudinal waves. In the following section we show how the first-order solution for the dispersion relation provides the real parts of the eigenvalues, thus allowing the study of the conditions for the oscillations to be amplified or damped.

IV. MARGINAL STABILITY CONDITIONS AND MODE MIXING

A. First-order solution

The quantities p_{j1}, u_{j1}, and w_{j1} $(j=1,2)$ have the same form as Eqs. (38)–(43). For simplicity, we do not write them explicitly, just implying that the constants $c_1,\ldots,c_4$ are substituted by the corresponding primed constants.

In the bottom and top boundary layers, using Eq. (20), we get that $\tilde{p}_{j0}$ $(j=1,2)$ do not depend on the vertical coordinate. Using the matching condition to the main bulk solution, we obtain

$$\tilde{p}_{10}=A_1,\quad \tilde{p}_{20}=A_2$$

with

$$A_1\equiv c_1\exp(-k)+c_2\exp(k)=-\frac{i\sqrt{\lambda}\rho\nu^{1/2}\coth(kh)}{\cosh(k)}c_6+\frac{\rho\lambda^2\coth(kh)}{k\cosh(k)}\eta+\frac{\omega_0^2[\coth(k)+\rho\coth(kh)]}{k\cosh(k)}\eta,$$

$$A_2\equiv c_3\exp(kh)+c_4\exp(-kh)=-\frac{i\sqrt{\lambda}\rho\nu^{1/2}}{\sinh(kh)}c_6+\frac{\rho\lambda^2}{k\sinh(kh)}\eta, \tag{65}$$

where the constants $c_1,\ldots,c_4$ have been expressed in terms of c_6 and η using Eqs. (44)–(46), (49), (52), and (53). Then Eq. (19) and BC (22) yield

$$\tilde{u}_{10}=-\frac{ikA_1}{\lambda}[1-\exp(-\sqrt{\lambda}\tilde{z}_1)],$$

$$\tilde{u}_{20}=-\frac{ikA_2}{\rho\lambda}[1-\exp(-\sqrt{\lambda}\nu^{-1/2}\tilde{z}_2)].$$

Using Eq. (18) and BC (22), we find $\tilde{w}_{j1}$, and then the matching condition between $w_{j0}+\epsilon w_{j1}$ and $\tilde{w}_{j0}+\epsilon\tilde{w}_{j1}$ yields

$$-c_1'\exp(-k)+c_2'\exp(k)=\frac{k}{\sqrt{\lambda}}A_1, \tag{66}$$

$$-c_3'\exp(kh)+c_4'\exp(-kh)=-\frac{k}{\sqrt{\lambda}}\nu^{1/2}A_2. \tag{67}$$

Returning to the interface boundary layer, let us first determine $\overline{p_{j1}}$. Equation (25) and BC (29) reduce to

$$\lambda\overline{w_{10}}=-\overline{p_{11\bar{z}}}+\overline{w_{10\bar{z}\bar{z}}},$$

$$\lambda\overline{w_{20}}=-\frac{1}{\rho}\overline{p_{21\bar{z}}}+\nu\overline{w_{20\bar{z}\bar{z}}}.$$

At $\bar{z}=0$,

$$\overline{p_{11}}-\overline{p_{21}}=2\overline{w_{10\bar{z}}}-2\rho\nu\overline{w_{20\bar{z}}}.$$

Then using Eqs. (50) and (51) and the matching condition between $p_{j0}+\epsilon p_{j1}$ and $\overline{p_{j0}}+\epsilon\overline{p_{j1}}$, we get

$$c_1'+c_2'-c_3'-c_4'=2(\rho\nu-1)ikc_6. \tag{68}$$

Equation (24) yields

$$\overline{u_{10}}=c_5'\exp(\sqrt{\lambda}\bar{z})-\frac{ik}{\lambda}(c_1+c_2), \tag{69}$$

$$\overline{u_{20}}=-\frac{ik}{\rho\lambda}(c_3+c_4). \tag{70}$$

Note that we define the constant c_6, appearing at the boundary layer exponential (48), as already containing enough approximations, as we earlier did with λ and η. That is why the expected exponential term is absent in Eq. (70).

Substituting Eqs. (69) and (70) into BC (28) and using the expression of $c_1,\ldots,c_4$ in terms of c_6 and η, we get

$$c_5'=D, \tag{71}$$

where

$$D\equiv\frac{ik}{\lambda}(c_1+c_2)-\frac{ik}{\rho\lambda}(c_3+c_4)=-\frac{k}{\sqrt{\lambda}}(1-\rho)\nu^{1/2}\coth(kh)c_6-i\lambda(1-\rho)\coth(kh)\eta+i\frac{\omega_0^2}{\lambda}[\coth(k)+\rho\coth(kh)]\eta. \tag{72}$$

To find $\overline{w_{j1}}$ we use Eq. (23) with Eqs. (69) and (70) and BC (27). The latter yields $\overline{w_{j1}}=0$ at $\bar{z}=0$ as η has been taken into account in the leading-order approximation. We get

$$\overline{w_{11}}=\frac{ikc_5'}{\sqrt{\lambda}}\,[1-\exp(\sqrt{\lambda}\overline{z})]-\frac{k^2}{\lambda}\,(c_1+c_2)\overline{z}, \tag{73}$$

$$\overline{w_{21}}=-\frac{k^2}{\rho\lambda}\,(c_3+c_4)\overline{z}. \tag{74}$$

The matching between $w_{j0}+\epsilon w_{j1}$ and $\overline{w_{j0}}+\epsilon\overline{w_{j1}}$ yields

$$\frac{k}{\lambda}\,(c_2'-c_1')=\frac{ik}{\sqrt{\lambda}}\,c_5', \tag{75}$$

$$\frac{k}{\rho\lambda}\,(c_4'-c_3')=0. \tag{76}$$

Now eliminating $c_1',\ldots,c_5'$ in the system (66)–(68), (71), (75), and (76) as done with the corresponding unprimed coefficients in the system (44)–(46), (49), (52), and (53), we get

$$2ik^2(\rho\nu-1)c_6+ik\sqrt{\lambda}D\,\coth(k)-\frac{k^2}{\sqrt{\lambda}}A_1\,\frac{1}{\sinh\,(k)}+\frac{k^2}{\sqrt{\lambda}}\,\nu^{1/2}A_2\,\frac{1}{\sinh\,(kh)}=0. \tag{77}$$

However, as we did not expand λ, η, and c_6, Eq. (77) cannot be used alone. Rather it must be taken together with Eq. (54), which is the corresponding result of the leading-order approximation.

For the temperature field, Eq. (26) together with Eqs. (73) and (74) yields

$$\overline{T_{11}}=-\frac{ikc_5'}{\lambda\sqrt{\lambda}}-\frac{ikc_5'}{\lambda\sqrt{\lambda}}\,\frac{\mathrm{Pr}}{1-\mathrm{Pr}}\exp(\sqrt{\lambda}\overline{z})+\frac{k^2}{\lambda^2}\,(c_1+c_2)\overline{z}+c_7'\,\exp(\sqrt{\lambda}\mathrm{Pr}^{1/2}\overline{z}), \tag{78}$$

$$\overline{T_{21}}=\kappa^{-1}\,\frac{k^2}{\rho\lambda^2}\,(c_3+c_4)\overline{z}+c_8'\,\exp(-\sqrt{\lambda}\mathrm{Pr}^{1/2}\chi^{-1/2}\overline{z}). \tag{79}$$

Determining c_7' and c_8' with the help of BC (31) and (32), which in the present approximation does not contain η, substituting Eqs. (69), (70), (78), and (79) into BC (30), and taking Eqs. (59), (71), and (72) into account, we get

$$D-\frac{mk^2}{\lambda^2}\,D\,\frac{1}{\mathrm{Pr}^{1/2}(1+\mathrm{Pr}^{1/2})(1+\kappa\chi^{-1/2})}=0. \tag{80}$$

Note again that Eq. (80) can be used only when combined with the previous order equation (60).

Finally, combining the zeroth- and first-order solutions, namely, Eq. (60) with Eq. (80) multiplied by ϵ and Eq. (54) with Eq. (77) multiplied by ϵ, and recalling the definitions (65) and (72), we get

$$a_{11}c+a_{21}\eta=0, \tag{81}$$

$$a_{12}c+a_{22}\eta=0, \tag{82}$$

with

$$a_{11}=1+\frac{mk^2}{\lambda^2}\,\frac{\chi^{1/2}\nu^{-1/2}-1}{(1+\rho\nu^{1/2})(1+\kappa\chi^{-1/2})(1+\mathrm{Pr}^{1/2})(\chi^{1/2}\nu^{-1/2}+\mathrm{Pr}^{1/2})}-\epsilon\,\frac{k}{\sqrt{\lambda}}\,\frac{(1-\rho)\,\nu^{1/2}}{1+\rho\nu^{1/2}}\,\coth(kh)\left[1-\frac{mk^2}{\lambda^2}\,\frac{1}{\mathrm{Pr}^{1/2}(\mathrm{Pr}^{1/2}+1)(1+\kappa\chi^{-1/2})}\right], \tag{83}$$

$$a_{21}=-\epsilon\,\frac{i}{1+\rho\nu^{1/2}}\left[(1-\rho)\lambda\,\coth(kh)-\frac{\omega_0^2}{\lambda}\,[\rho\,\coth(kh)+\coth(k)]\right]\left[1-\frac{mk^2}{\lambda^2}\,\frac{1}{\mathrm{Pr}^{1/2}(\mathrm{Pr}^{1/2}+1)(1+\kappa\chi^{-1/2})}\right], \tag{84}$$

$$a_{12}=-ik\sqrt{\lambda}[\rho\nu^{1/2}\,\coth(kh)-\coth(k)]+\epsilon ik^2\left[2(\rho\nu-1)-(1-\rho)\,\nu^{1/2}\,\coth(k)\coth(kh)+\rho\nu^{1/2}\,\frac{\coth(kh)}{\sinh(k)\cosh(k)}-\rho\nu\,\frac{1}{\sinh^2(kh)}\right], \tag{85}$$

$$a_{22}=[\rho\,\coth(kh)+\coth(k)](\lambda^2+\omega_0^2)+\epsilon\,\frac{k}{\sqrt{\lambda}}\left[\lambda^2(1-\rho)\coth(k)\coth(kh)-\omega_0^2[\rho\,\coth(kh)+\coth(k)]\coth(k)-\rho\lambda^2\,\frac{\coth(kh)}{\sinh(k)\cosh(k)}-\omega_0^2\,\frac{\coth(kh)+\coth(k)}{\sinh(k)\coth(k)}+\rho\nu^{1/2}\lambda^2\,\frac{1}{\sinh^2(kh)}\right]. \tag{86}$$

For simplicity, we have omitted the subscript for the constant c_6. The results (81)–(86) are enough for the purpose of the present paper.

B. Stability analysis of (oscillatory) modes

Satisfying the solvability condition

$$a_{11}a_{22}-a_{12}a_{21}=0, \tag{87}$$

we get an approximate dispersion relation. The leading-(zeroth-) order approximation was studied in Sec. III B, where it was shown that two modes, transverse and longitudinal, exist. However, only the imaginary part of the eigenvalues, and hence their corresponding frequencies, was obtained. To assess the stability of these two modes we need to calculate the real part, which is ϵ times smaller. This quantity is obtained in the first-order approximation. Thus we expand λ as Eq. (37), implying that λ_0 is given by Eq. (62) for the transverse mode and by Eq. (63) for the longitudinal mode, respectively. Then Eq. (87), taken at order ϵ, yields the following equations for λ_1:

$$\begin{aligned}
&2\lambda_1\left(1-\frac{m}{m_{\rm res}}\right)[\rho\,\coth(kh)+\coth(k)]+k\sqrt{\lambda_0}\left(1-\frac{m}{m_{\rm res}}\right)\\
&\quad\times\left[\coth(k)[\coth(k)+\coth(kh)]+\frac{1}{\sinh^2(k)}\right.\\
&\quad\left.+\frac{\rho\nu^{1/2}}{\sinh^2(kh)}\right]\\
&\quad+k\sqrt{\lambda_0}\left[1+\frac{m}{m_{\rm res}}\,\frac{(1+\rho\nu^{1/2})(\chi^{1/2}\nu^{-1/2}+{\rm Pr}^{1/2})}{{\rm Pr}^{1/2}(\chi^{1/2}\nu^{-1/2}-1)}\right]\\
&\quad\times\frac{\rho\nu^{1/2}\,\coth(kh)-\coth(k)}{1+\rho\nu^{1/2}}\,[\coth(k)+\coth(kh)]=0
\end{aligned} \tag{88}$$

for the transverse mode and

$$\begin{aligned}
&2\lambda_1\left(1-\frac{m_{\rm res}}{m}\right)[\rho\,\coth(kh)+\coth(k)]+k\sqrt{\lambda_0}\left[\frac{1}{1+\rho\nu^{1/2}}\right.\\
&\left.+\frac{\chi^{1/2}\nu^{-1/2}+{\rm Pr}^{1/2}}{{\rm Pr}^{1/2}(\chi^{1/2}\nu^{-1/2}-1)}\right]\left[-(1-\rho)\right.\\
&\times(1+\nu^{1/2})\coth(k)\coth(kh)+\frac{m_{\rm res}}{m}\,[\nu^{1/2}\,\coth(kh)\\
&\left.-\coth(k)][\rho\,\coth(kh)+\coth(k)]\right]=0
\end{aligned} \tag{89}$$

for the longitudinal mode. $m_{\rm res}$ was defined in Eq. (64). As for both modes λ_0 is purely imaginary (we only consider the case when the longitudinal mode is oscillatory), then $\sqrt{\lambda_0}=(1\pm i)|\lambda_0|^{1/2}/\sqrt{2}$, where (for positive k) ${\rm Im}(\lambda_0)<0$ and ${\rm Im}(\lambda_0)>0$ correspond to right and left propagating waves, respectively.

The sign of ${\rm Re}(\lambda_1)$ determines whether the corresponding wave is damped or amplified. In particular, at $m=0$, Eq. (88) yields the damping coefficient for capillary-gravity waves in the usual, isothermal situation. ${\rm Re}(\lambda_1)=0$ defines the condition of marginal stability, providing the marginal curves ''m versus k.'' Imposing ${\rm Re}(\lambda_1)=0$ in Eqs. (88) and (89), we get

$$\begin{aligned}
m_{\rm tr}=m_{\rm res}&\left\{\frac{\rho\nu^{1/2}[\coth(k)+\coth(kh)]^2}{1+\rho\nu^{1/2}}+\frac{1}{\sinh^2(k)}\right.\\
&\left.+\frac{\rho\nu^{1/2}}{\sinh^2(kh)}\right\}\left\{\coth(k)[\coth(k)+\coth(kh)]+\frac{1}{\sinh^2(k)}\right.\\
&+\frac{\rho\nu^{1/2}}{\sinh^2(kh)}+\frac{\chi^{1/2}\nu^{-1/2}+{\rm Pr}^{1/2}}{{\rm Pr}^{1/2}(\chi^{1/2}\nu^{-1/2}-1)}\,[\coth(k)\\
&\left.-\rho\nu^{1/2}\,\coth(kh)][\coth(k)+\coth(kh)]\right\}^{-1}
\end{aligned} \tag{90}$$

for the transverse mode and

$$m_{\rm long}=m_{\rm res}\,\frac{[\nu^{1/2}\,\tanh(k)-\tanh(kh)][\rho\,\coth(kh)+\coth(k)]}{(1-\rho)(1+\nu^{1/2})} \tag{91}$$

for the longitudinal mode, where $m_{\rm res}$ is defined in Eq. (64).

Note that the marginal condition (91) is valid only if

$$E_1\equiv\nu^{1/2}\,\tanh(k)-\tanh(kh)>0. \tag{92}$$

Otherwise the longitudinal mode (63) is not oscillatory. Depending on the values of ν and h, the inequality (92) can hold for all k, for some interval of k, or else for no k at all. Indeed, (i) if $1<h<\nu^{1/2}$ or $h<1<\nu^{1/2}$, we have $E_1>0$, i.e., $m_{\rm long}$ exists for all k; (ii) if $\nu^{1/2}<1<h$ or $\nu^{1/2}<h<1$, then $E_1<0$, i.e., there are no marginal states for the longitudinal mode. (iii) if $1<\nu^{1/2}<h$, the marginal curve occupies only the interval $k>k_0$, where $k_0\neq 0$ is the root of E_1, which does not exist in the first two cases; and finally, (iv) if $h<\nu^{1/2}<1$, the marginal states exist only for $k<k_0$.

Due to the condition (92), the signs of $m_{\rm long}$ and $m_{\rm res}$ always coincide. At the same time, in view of Eq. (64), they are defined by the sign of $\chi^{1/2}\nu^{-1/2}-1$. Thus it is clear how $m_{\rm long}$ behaves. As for $m_{\rm tr}$ [Eq. (90)], no such simple criteria exist.

The possibility of extending the longitudinal marginal curve up to $m_{\rm long}=0$ [cases (iii) and (iv) above] demands clarification. The same occurs when at $m\to 0$ Eq. (89) yields in some cases a persisting instability for the longitudinal mode. This can be understood in the following way. The oscillatory instability studied here is associated with interfacial deformations at large Galileo number ($G\gg 1$) and consequently with high Marangoni numbers ($m\sim 1$, hence $M\sim G\gg 1$). However, in the two-layer system, the oscillatory instability can appear even if the interface is not deformable (for $M\sim 1\ll G$). It is having this fact in mind that our results for the longitudinal mode should be considered. For example, the fact that $m_{\rm long}\to 0$ at some $k\to k_0$ is an indication that there is a vertical asymptote of a ''low-M'' oscillatory marginal curve at the same $k=k_0$. Analogously, if the longitudinal mode remains amplified for some interval of k at $m\to 0$, it means that there necessarily exists an amplified oscillatory mode in the Bénard-Marangoni problem with an

undeformable interface, provided M is taken large enough and has the same sign as needed for the mode (63) to be oscillatory.

λ_1 diverges when calculated using Eqs. (88) or (89) at $m \to m_{\rm res}$. Thus an improved asymptotic analysis in the vicinity of the resonance curve is needed. First of all, when the coefficient of λ_1 becomes small, one must also take into account the quadratic term ($\sim \lambda_1^2$) when deriving an equation for λ_1 from Eq. (87). At $m = m_{\rm res}$ it becomes the leading-order term containing the correction to the eigenvalue, λ_1. Consequently, the following scaling is appropriate here:

$$\lambda = \Lambda_0 + \epsilon^{1/2}\Lambda_1 + \cdots , \tag{93}$$

where $\Lambda_0 \equiv \pm i\omega_0$ coincides with λ_0 for the transverse mode, while

$$\delta(m) \equiv \frac{m - m_{\rm res}}{m_{\rm res}}\, \epsilon^{-1/2} \sim 1. \tag{94}$$

Note that the correction to the eigenvalue becomes asymptotically higher near the resonance. Finally, using Eqs. (93) and (94) in Eq. (87), we derive the equation for Λ_1,

$$\frac{4}{\Lambda_0}\,\Lambda_1^2 - 2\,\delta(m)\Lambda_1 + Q = 0, \tag{95}$$

with

$$Q \equiv k\sqrt{\Lambda_0}\left[1 + \frac{(1+\rho\nu^{1/2})(\chi^{1/2}\nu^{-1/2} + {\rm Pr}^{1/2})}{{\rm Pr}^{1/2}(\chi^{1/2}\nu^{-1/2} - 1)}\right] \times \frac{\rho\nu^{1/2}\,\coth(kh) - \coth(k)}{1 + \rho\nu^{1/2}}\,\frac{\coth(k) + \coth(kh)}{\coth(k) + \rho\,\coth(kh)}.$$

Here we assume that $Q \sim 1$ and thus we exclude from consideration a small interval of k around k_*, where k_* is a root of

$$E_2 \equiv \rho\nu^{1/2}\,\coth(kh) - \coth(k), \tag{96}$$

where it exists. This peculiar case will be treated later on (see Sec. V).

Near resonance, the zeroth-order eigenvalues for the two modes coincide and a difference appears only in the first-order approximation. Accordingly, Eq. (95) has two solutions for Λ_1.

Before providing the solution, let us point out some basic details concerning Λ_1 satisfying Eq. (95). First, there are no values of the parameters for which purely imaginary solutions exist. Thus there are no marginally stable states in the vicinity of the resonance point. Second, for $m = m_{\rm res}$, Eq. (95) implies that Λ_1^2 is a complex quantity. Then one of the eigenvalues always has a positive real part, while the real part of the other is always negative. In the absence of marginally stable states, the continuity demands that this holds in the vicinity of the resonance point. Consequently, the resonance occurs only when one of the two modes is unstable.

The solution of Eq. (95) is

$$\Lambda_1 = \frac{\Lambda_0}{4}\left[\delta(m) \pm \sqrt{\delta^2(m) - \frac{4}{\Lambda_0}\,Q}\right]. \tag{97}$$

In the region $|\delta(m)| \gg 1$, $\Lambda_0 + \epsilon^{1/2}\Lambda_1$ should match with $\lambda_0 + \epsilon\lambda_1$ for the transverse and longitudinal modes, taken at $m \to m_{\rm res}$. λ_0 is defined in Eqs. (62) and (63) and λ_1 in Eqs. (88) and (89). Let us study the limit $|\delta(m)| \gg 1$ in Eq. (97). Taking, for illustration, ''positive'' branch of the solution, we have

$$\Lambda_1 \cong \frac{1}{2}\,\frac{Q}{\delta(m)} + \cdots \tag{98}$$

for $\delta(m) < 0$ and

$$\Lambda_1 \cong \frac{\Lambda_0}{2}\,\delta(m) - \frac{1}{2}\,\frac{Q}{\delta(m)} + \cdots \tag{99}$$

for $\delta(m) > 0$.

Equation (98) coincides (up to the factor $\epsilon^{1/2}$) with the result given by Eq. (88), for the transverse mode, in the limit $m \to m_{\rm res}$. The second term on the right-hand side of Eq. (99) is identical (up to the same factor) to the result provided by Eq. (89) for the longitudinal mode at $m \to m_{\rm res}$, while the first term accounts for the fact that the leading-order frequencies for the longitudinal mode become different from ω_0 away from the resonant curve. Thus the positive branch of Eq. (97) tends to the transverse eigenvalue at $|m - m_{\rm res}| \gg \epsilon^{1/2}$, $m < m_{\rm res}$, and to the longitudinal eigenvalue at $|m - m_{\rm res}| \gg \epsilon^{1/2}$, $m > m_{\rm res}$. Analogously, one can show that the opposite holds for the ''negative'' branch.

Thus there is a continuous transition from the transverse mode to the longitudinal one, and vice versa, around the resonance curve, where mode mixing occurs. The salient features of this transition are (i) conservation and alternation of the sign of Re(λ), i.e., at each stage of the transition, Re(λ) >0 for one of the (mixed) modes and Re(λ)<0 for the other, and (ii) Re(λ) becomes asymptotically larger near the resonance, although still Re(λ)$\ll$Im(λ).

Shown in Figs. 1 and 2 are some representative cases illustrating the behavior of the marginal curves for the transverse (solid line marked 1) and longitudinal (solid line marked 2) modes, as well as the resonance curve (dot-dashed line). In view of symmetry, we plot them only for $k > 0$. The parameter values used are indicated in the figure captions. As earlier shown, in some cases the longitudinal marginal curve does not exist. These three curves, as well as the axis $m = 0$, subdivide the semiplane $\{k > 0, m\}$ into regions, according to the different (damping or amplification) status of transverse and longitudinal waves. We have expressed this in Figs. 1 and 2 with the help of vertical arrows: The first arrow corresponds to the transverse mode and the second one to the longitudinal mode. An arrow pointing up means that the corresponding mode is amplified, otherwise it denotes a damped mode. In the quadrant $m > 0$, or $m < 0$, where the longitudinal mode is not oscillatory, the second arrow is replaced by an asterisk.

Given a particular diagram of marginal and resonance curves, there is no need to refer to Eqs. (88) and (89) to establish the damping or amplification status in each region (i.e., setting arrows and asterisks). Rather, this can be *unambiguously* established with the help of the earlier established facts: (i) The transverse mode is always damped in the regions adjacent to $m = 0$, (ii) the sign of Re(λ) is conserved

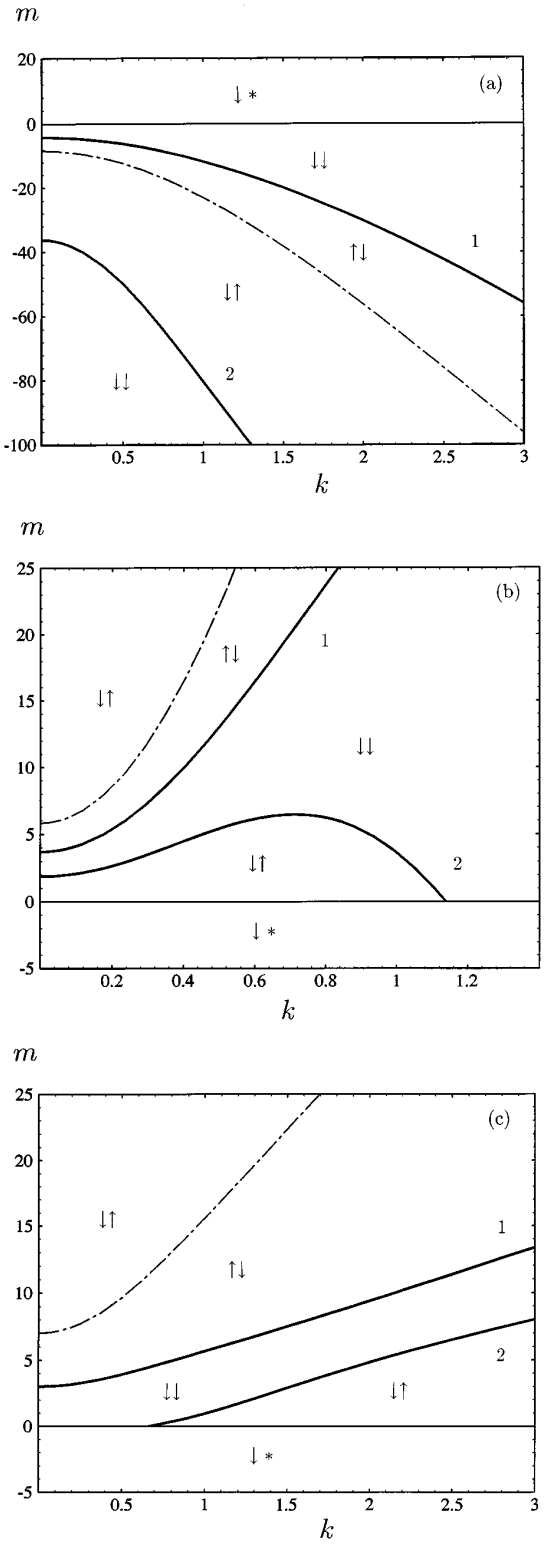

FIG. 1. Marginal curves for the transverse [solid line 1, Eq. (90)] and longitudinal [solid line 2, Eq. (91)] waves and the resonance curve [dot-dashed line, Eq. (64)] for (a) $h=0.2$, $\rho=0.5$, $\nu=4.5$, $\chi=1.0$, $\kappa=0.5$, $B=1.0$, and Pr$=6.0$; (b) $h=0.5$, $\rho=0.5$, $\nu=0.4$, $\chi=2.0$, $\kappa=0.5$, $B=0.17$, and Pr$=6.0$; and (c) $h=1.2$, $\rho=0.5$, $\nu=1.3$, $\chi=4.0$, $\kappa=0.5$, $B=1.0$, and Pr$=2.0$. In each region the arrows indicate whether the transverse (first arrow) and longitudinal (second arrow) are amplified (arrow up) or damped (arrow down). When the longitudinal mode is not oscillatory, the second arrow is replaced by an asterisk.

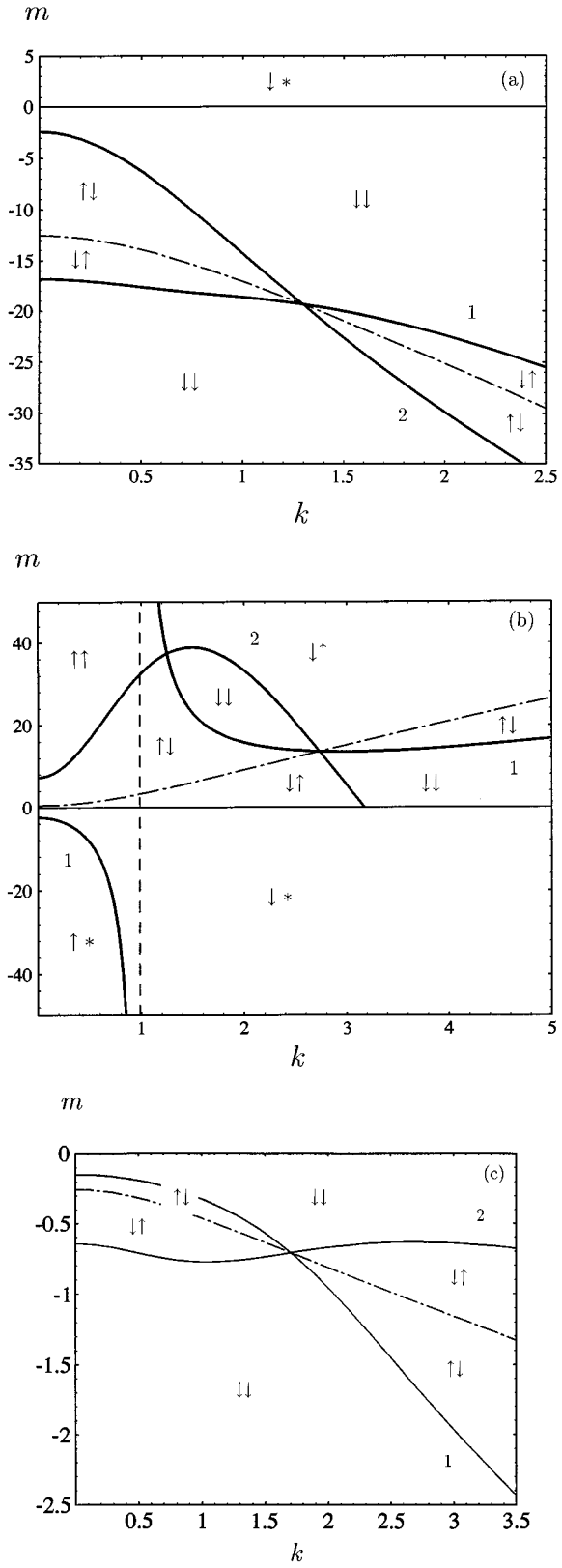

FIG. 2. Same as in Fig. 1 for (a) $h=1.6$, $\rho=0.65$, $\nu=3.0$, $\chi=0.5$, $\kappa=0.3$, $B=3.0$, and Pr$=6.0$; (b) $h=0.45$, $\rho=0.95$, $\nu=0.8$, $\chi=2.0$, $\kappa=0.5$, $B=3.0$, and Pr$=2.0$; and (c) $h=0.9$, $\rho=0.95$, $\nu=1.05$, $\chi=0.4$, $\kappa=1.0$, $B=15.0$, and Pr$=0.01$. Note the resonant intersection of the transverse and longitudinal marginal curves in the examples.

and alternates around the resonance curve, (iii) crossing a marginal curve, we change from damping to amplification or vice versa for the corresponding mode, and (iv) the longitudinal mode is oscillatory only in the semiplane containing the resonance curve (and the longitudinal marginal curve, when it exists). In each case, there is only one set of arrows and asterisks that does not contradict (i)–(iv).

The marginal curves can intersect (as in the examples of Fig. 2) either *nonresonantly* or *resonantly*. In the latter case, the resonance curve also passes through the point of intersection. It can be shown that the necessary and sufficient condition for the existence of a resonant intersection is that E_2, defined in Eq. (96), vanishes at some $k=k_*$. Thus we conclude that *resonant* intersection occurs if and only if either $1<\rho\nu^{1/2}<h$ or $h<\rho\nu^{1/2}<1$.

A further improved asymptotic study (see the next section) is needed to properly account for the ϵ vicinity of the resonant intersection point $\{k_*,m_*\}$, where m_* is $m_{\rm res}$, $m_{\rm tr}$, or, equivalently, $m_{\rm long}$ evaluated at $k=k_*$. None of the results (88)–(91), nor Eq. (97), is correct there. Indeed, at $k\to k_*$, $m\to m_*$, no order unity terms exist in the matrix elements (83)–(86). Thus the leading order determinant (87) is of order ϵ^2, while the results (88), (89), and (97) have been obtained evaluating the determinant (87) in the order ϵ. On the other hand, for the purpose of studying the vicinity of the point $k=k_*$, $m=m_*$, as there are no terms of order unity, we do not need to calculate ϵ^2 contributions to the coefficients (83)–(86).

V. DETAILS OF THE MARGINAL CURVES NEAR THE RESONANT INTERSECTION

Considering the vicinity of the resonant intersection point, we impose

$$k=k_*+\epsilon\Delta(k)+\cdots,\quad m=m_*+\epsilon\Delta(m)+\cdots,$$
$$\lambda=i\omega_*+\epsilon\Delta(\lambda)+\cdots, \tag{100}$$

where ω_* is ω_0 taken at $k=k_*$. After using Eq. (100) in Eqs. (83)–(86), Eq. (87) becomes

$$q_2\left[\Delta(\lambda)+\frac{\beta\Delta(k)}{2i\omega_*}\right]^2+q_1\left[\Delta(\lambda)+\frac{\beta\Delta(k)}{2i\omega_*}\right]+q_0=0, \tag{101}$$

with

$$q_2=4(1+\nu^{-1/2})\coth(k_*),$$

$$q_1=2i\omega_*(1+\nu^{-1/2})\coth(k_*)\left(-\frac{\Delta(m)}{m_*}-2\frac{\Delta(k)}{k_*}+\beta\frac{\Delta(k)}{\omega_*^2}\right)-2k_*\sqrt{i\omega_*}\,\frac{(1-\rho)(1+\nu^{-1/2})}{\rho(1+\rho\nu^{1/2})}\coth^2(k_*)B+2k_*\sqrt{i\omega_*}(1+\rho\nu^{1/2})\left(\frac{2}{\rho\nu^{1/2}}\coth^2(k_*)-1\right),$$

$$q_0=\frac{k_*i\omega_*\sqrt{i\omega_*}}{\rho\nu^{1/2}}\coth(k_*)B\alpha\Delta(k)$$
$$-k_*^2i\omega_*\coth(k_*)B\left(3\frac{\rho\nu-1}{\rho\nu^{1/2}}-\frac{1-\rho}{\rho}\right)$$
$$+k_*i\omega_*\sqrt{i\omega_*}(1+\rho\nu^{1/2})\left(\frac{2}{\rho\nu^{1/2}}\coth^2(k_*)-1\right)$$
$$\times\left(-\frac{\Delta(m)}{m_*}-2\frac{\Delta(k)}{k_*}+\beta\frac{\Delta(k)}{\omega_*^2}\right),$$

where α is the slope of E_2 [Eq. (96)] at $k=k_*$, β is the same for ω_0^2, and

$$B\equiv 1+\frac{(1+\rho\nu^{1/2})(\chi^{1/2}\nu^{-1/2}+\mathrm{Pr}^{1/2})}{\mathrm{Pr}^{1/2}(\chi^{1/2}\nu^{-1/2}-1)}.$$

Looking for the marginally stable states described by Eq. (101), we set $\mathrm{Re}[\Delta(\lambda)]=0$. Then $\mathrm{Im}[\Delta(\lambda)]=-\mathrm{Im}(q_0)/\mathrm{Re}(q_1)$, and finally eliminating $\Delta(\lambda)$, we get

$$-q_2\,\mathrm{Im}^2(q_0)+\mathrm{Im}(q_1)\mathrm{Im}(q_0)\mathrm{Re}(q_1)+\mathrm{Re}(q_0)\mathrm{Re}^2(q_1)=0.$$

Alternatively, we have

$$-q_2\,\mathrm{Im}^2(q_0)+[\mathrm{Im}(q_1)-\mathrm{sgn}(\omega_*)\mathrm{Re}(q_1)]\mathrm{Im}(q_0)\mathrm{Re}(q_1)+[\mathrm{Re}(q_0)+\mathrm{sgn}(\omega_*)\mathrm{Im}(q_0)]\mathrm{Re}^2(q_1)=0. \tag{102}$$

After substituting the expressions for q_0, q_1, and q_2, Eq. (102), as expected, depends only on the absolute value of ω_*, rather than on its sign.

Equation (102) is a quadratic equation for $\Delta(k)$ and $\Delta(m)$. In the plane $\Delta(m)$ versus $\Delta(k)$ it defines a hyperbolic marginal curve. Some examples are shown in Fig. 3 (solid line) for the same parameter combinations as in Fig. 2, where the resonant intersection occurs. The dashed lines, marked 1 and 2, and dot-dashed lines correspond to the direct continuations of $m_{\rm tr}$, $m_{\rm long}$, and $m_{\rm res}$, respectively, linearized in the vicinity of the resonant intersection point. The axes of the hyperbole are naturally parallel to the linearizations of $m_{\rm tr}$ and $m_{\rm long}$. They provide a successful leading-order matching between the marginal curves in the vicinity and far away from the resonant intersection point. The appearance of the shift is due to the use of different orders of approximation when deriving the results (90), (91) (ϵ^1 approximation), and (102) (ϵ^2 approximation). Accordingly, the shift should be taken into account in the next-order matching, between Eq. (102) and the next-order correction to the marginal curves (90) and (91). This task is beyond the scope of the present paper.

Thus, studying the detailed structure of marginal curves near the point $\{k_*,m_*\}$, it appears that in fact they do not intersect. Actually, there is rounding off of a pair of two opposite corners, accompanied by the formation of a gap between two separate branches of the marginal curve. A simple criterion can be established concerning which one of the two pairs of opposite corners is rounded off, the one containing the resonance curve (first possibility) or the other (second possibility). Indeed, considering the points along the resonance curve, which in terms of $\Delta(m)$ and $\Delta(k)$ can be written as

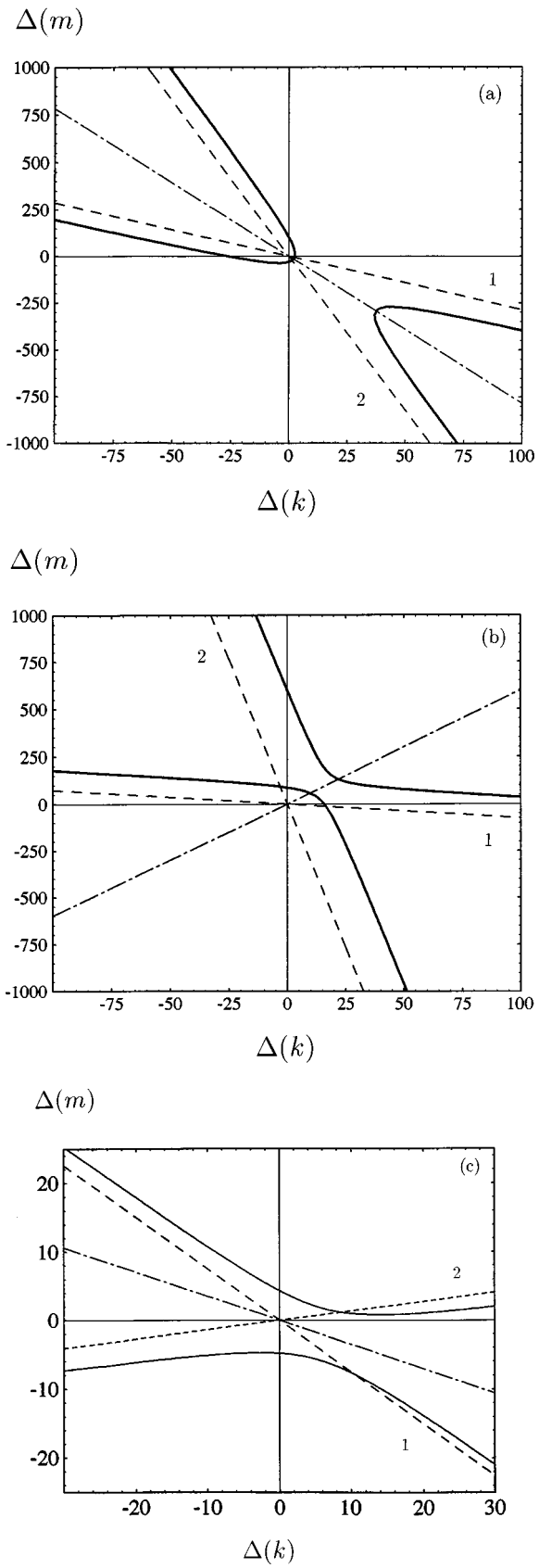

FIG. 3. Enlarged view of the resonant intersection of marginal curves. The cases (a)–(c) are the same as in Fig. 2. Marginal curves (solid line), direct continuations of the resonance curve (dot-dashed line), and transverse (dashed line 1) and longitudinal (dashed line 2) marginal curves of Fig. 2.

$$-\frac{\Delta(m)}{m_*}-2\frac{\Delta(k)}{k_*}+\beta\frac{\Delta(k)}{\omega_*^2}=0,$$

we get $\mathrm{Im}(q_1)-\mathrm{sgn}(\omega_*)\mathrm{Re}(q_1)=0$, i.e., the second term on the left-hand side of Eq. (102) is zero. Then, as $q_2>0$, Eq. (102) may have two solutions for $\Delta(k)$, corresponding to the intersection of the resonance curve with the two branches of the marginal curve, only if $\mathrm{Re}(q_0)+\mathrm{sgn}(\omega_*)\mathrm{Im}(q_0)>0$, i.e., if

$$E_3\equiv\frac{3\rho\nu^{1/2}+\rho-3\nu^{-1/2}-1}{\chi^{1/2}\nu^{-1/2}-1}<0.$$

Thus, if $E_3<0$, the first possibility is realized, while if $E_3>0$, the second possibility occurs, in accordance with the cases shown in Fig. 3.

VI. CONCLUDING REMARKS

The linear analysis of the Bénard-Marangoni oscillatory instability in a system of two horizontal liquid layers of finite depth separated by a free deformable interface and subjected to a vertical temperature gradient has been carried out. Assuming that the Galileo number is large, while the capillary number is small, and using the boundary layer approximation, we have asymptotically studied the high Marangoni number branches of instability, associated with interface deformations, and found that they can be described in terms of (high-frequency) transverse (capillary-gravity) and longitudinal wave modes.

The leading-order dispersion relation enabled us to calculate the frequencies of both the transverse (62) and the longitudinal (63) waves. The longitudinal mode does not appear always oscillatory. It is so only when $m(\chi-\nu)>0$, i.e., if the heating is from above for $\chi>\nu$ and if the heating is from below for $\chi<\nu$. We have also obtained the damping or amplification rates [Eqs. (88) and (89)], which are always asymptotically smaller than the frequencies. The marginal stability conditions for the both modes, represented in terms of marginal curves ''modified Marangoni number versus wave number,'' $\{m,k\}$ [Eqs. (90) and (91) and Figs. 1 and 2], have been analyzed.

The possibility of resonance between transverse and longitudinal waves has been studied in detail. It occurs when the frequencies given by Eqs. (62) and (63) approach each other, hence defining the resonance curve (64). Near resonance, mode mixing is expected. As a consequence of the mixing, the transverse mode is converted into the longitudinal one and vice versa [Eq. (95)]. At this transition, the damping or amplification rate becomes asymptotically higher than away from the resonance. We have shown that, given a diagram of the marginal and resonance curves (Figs. 1 and 2), one can unambiguously determine in which regions of the plane $\{m,k\}$ a given mode is damped or amplified.

It was also found that there can exist nonresonant and resonant intersections of the transverse and longitudinal marginal curves. The necessary and sufficient condition for the existence of the resonant intersection is that E_2 [Eq. (96)] vanishes at some wave number. Details of the behavior of marginal curves in a small vicinity of the resonant intersection point have been analyzed (Fig. 3).

The results for the *longitudinal mode* obtained here permit

some conclusions and predictions concerning the structure of the low Marangoni number branches for oscillatory instability in the two-layer problem with undeformable separating interface. Indeed, the results found here, when taken in the limit $|m| \ll 1$, should match the corresponding results obtained for the problem with a flat, undeformable interface taken in the limit $|M| \gg 1$. For example, the eigenvalue $\lambda_0 + \epsilon\lambda_1$, with λ_0 and λ_1 defined in Eqs. (63) and (91) taken in the limit of small m [Eq. (59)], provides the asymptotics of the corresponding eigenvalue in the problem with flat interface at large M. In this way, one can easily study for which cases $\mathrm{Re}(\lambda_1) > 0$, which helps orientation in the parameter space. Take, e.g., the possibility for the longitudinal marginal curve to approach zero at some $k = k_0$, where k_0 is a root, if any, of E_1 [Eq. (92)]. In this case, one should expect a vertical asymptote to the low Marangoni oscillatory marginal curve at the same $k = k_0$. It turns out that the existence and behavior of this asymptote is governed by only two parameters ν and h entering E_1.

ACKNOWLEDGMENTS

This work was supported by the Fundación ''Ramón Areces'' (Spain), by the Fundación BBV (Programa Catedra, Cambridge), by INTAS Grant No. 94-242, by DGICYT (Spain) under Grant No. PB93-81, by the Human Capital and Mobility Program of the European Union (Network No. ERBCHRXCT960010), by the European Space Agency Prodex Programme, and by the Belgian Program on Interuniversity Poles of Attraction (PAI 4-06) initiated by the Belgian State, Prime Minister's Office, Federal Office for Scientific, Technical and Cultural Affairs.

[1] L. E. Scriven and C. V. Sternling, Nature (London) **187**, 186 (1960).
[2] *Physicochemical Hydrodynamics. Interfacial Phenomena*, edited by M. G. Velarde (Plenum, New York, 1988).
[3] E. L. Koschmieder, *Bénard Cells and Taylor Vortices* (Cambridge University Press, Cambridge, 1993).
[4] J. R. Pearson, J. Fluid Mech. **4**, 489 (1958).
[5] A. Vidal and A. Acrivos, Phys. Fluids **9**, 615 (1966).
[6] C. V. Sternling and L. E. Scriven, AIChE. J. **5**, 514 (1959).
[7] J. Reichenbach and H. Linde, J. Colloid Interface Sci. **84**, 433 (1981).
[8] I. B. Simanovskii and A. A. Nepomnyashchy, *Convective Instabilities in Systems with Interface* (Gordon and Breach, New York, 1993).
[9] Ph. Géoris, M. Hennenberg, I. B. Simanovskii, A. A. Nepomnyashchy, I. I. Wertgeim, and J. C. Legros, Phys. Fluids A **5**, 1575 (1993).
[10] P. Colinet, Ph. Géoris, J. C. Legros, and G. Lebon, Phys. Rev. E **54**, 514 (1996).
[11] J. L. Castillo and M. G. Velarde, Phys. Lett. **66A**, 489 (1978).
[12] J. L. Castillo and M. G. Velarde, J. Non-Equilib. Thermodyn. **5**, 111 (1980).
[13] J. L. Castillo and M. G. Velarde, J. Fluid Mech. **125**, 463 (1982).
[14] S. Van Vaerenbergh, P. Colinet, and J. C. Legros, in *Capillarity Today* , edited by G. Pétré and A. Sanfeld, (Springer-Verlag, Berlin, 1991), pp. 281–294.
[15] M. Takashima, J. Phys. Soc. Jpn. **50**, 2751 (1981).
[16] L. D. Landau and E. M. Lifshitz, *Fluid Mechanics* (Pergamon, Oxford, 1987).
[17] E. B. Levchenko and A. L. Chernyakov, Zh. Eksp. Teor. Fiz. **81**, 202 (1981) [Sov. Phys. JETP **54**, 102 (1981)].
[18] P. L. Garcia-Ybarra and M. G. Velarde, Phys. Fluids **30**, 1649 (1987).
[19] X. L. Chu and M. G. Velarde, Phys. Chem. Hydrodyn. **10**, 727 (1988).
[20] M. G. Velarde and X. L. Chu, Phys. Scr. **T25**, 231 (1989).
[21] M. Hennenberg, X. L. Chu, A. Sanfeld, and M. G. Velarde, J. Colloid Interface Sci. **150**, 7 (1992).
[22] A. Ye. Rednikov, P. Colinet, M. G. Velarde, and J. C. Legros (unpublished).
[23] M. G. Velarde and X. L. Chu, Phys. Lett. A **131**, 430 (1988).
[24] M. G. Velarde and X. L. Chu, Nuovo Cimento D **11**, 709 (1989).
[25] X. L. Chu and M. G. Velarde, J. Colloid Interface Sci. **131**, 471 (1989).
[26] J. Lucassen, Trans. Faraday Soc. **64**, 2221 (1968).
[27] E. H. Lucassen-Reynders and J. Lucassen, Adv. Colloid Interface Sci. **2**, 347 (1969).
[28] J. C. Earnshaw and A. C. McLaughlin, Proc. R. Soc. London, Ser. A **440**, 519 (1993).
[29] J. C. Earnshaw and E. McCoo, Phys. Rev. Lett. **72**, 84 (1994).
[30] See, e.g., A. H. Nayfeh, *Introduction to Perturbation Techniques* (Wiley, New York, 1993).